JOURNAL OF COMPUTATIONAL PHYSICS 79, 200–208 (1988)

A Finite Element Code for the Simulation of One-Dimensional Vlasov Plasmas. II. Applications

S. I. ZAKI, T. J. M. BOYD*, AND L. R. T. GARDNER

*Departments of Applied Mathematics and Computation, and * Physics, University of Wales, Bangor LL57 2UW, Wales*

Received March 20, 1987; revised November 9, 1987

The finite element method for solving the Vlasov–Poisson equations described in Part I has been tested on a number of standard problems—linear and nonlinear Landau damping of plasma waves, the two-stream and bump-on-tail instabilities, and the accuracy of the method verified by comparison with results from other methods. © 1988 Academic Press, Inc.

1. INTRODUCTION

In Part I we presented a finite element scheme providing for a numerical solution of the Vlasov–Poisson equations. In Part II we turn to some applications of the scheme, beginning with a set of well-understood problems which we have used to test the code throughly. To this end we have examined in turn the damping of an electrostatic plasma wave and the two-stream and bump-on-tail instabilities. Detailed comparisons of the finite element solutions show very good agreement indeed with various results in the literature. In particular, in Section 2a we compare results on *linear Landau damping* not only with standard theory but with the numerical results of Cheng and Knorr [1] and Canosa, Gazdag, and Fromm [2]; the finite-element results for *nonlinear Landau damping* are shown to agree well with those published by Cheng and Knorr. In Sections 2b and 2c we consider the two stream and bump-on-tail instabilities and show that the finite element results reproduce satisfactorily earlier results of Cheng and Knorr [1], Armstrong and Montgomery [3], and Klimas [4].

2. TESTS OF FEM VLASOV CODE

(a) *Damping of Electrostatic Waves*

In this section we apply the results of Part I to retrieve the classical and well-understood linear and nonlinear Landau damping of plasma waves. We solve the

0021-9991/88 $3.00

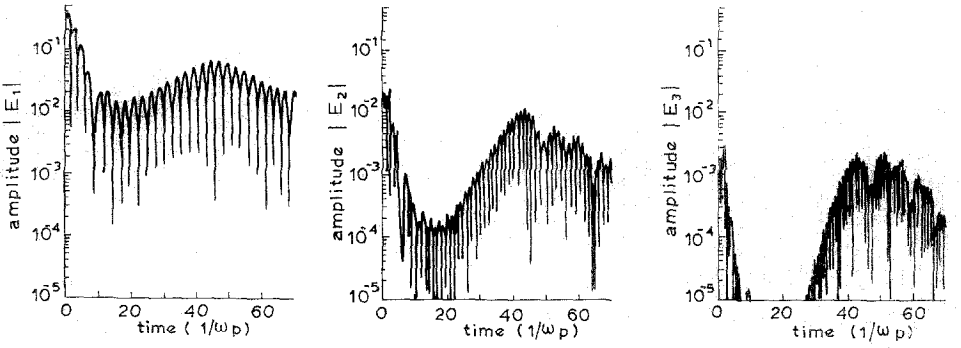

FIG. 1. Evolution of the first tree Fourier modes of an electric field.

dimensionless Vlasov–Poisson equations taking an initial electron distribution function of the form

$$f_0(x, v, o) = f_0(v)(1 + A \cos Kx)$$
$$f_0(v) = (1/\sqrt{2\pi}) \exp(-v^2/2), \tag{1}$$

where K is the wave number and A is the amplitude of the initial perturbation. We examined the evolution of the amplitude of the electric field for $K = 0.3$, and

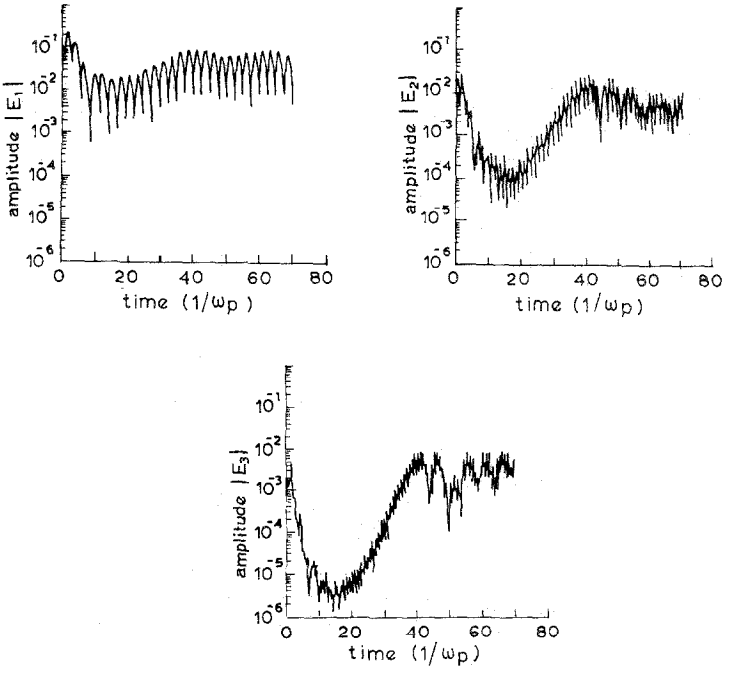

FIG. 2. Evolutions of the first three Fourier mode amplitudes obtained by Cheng and Knorr [1].

$A = 0.0159$. After the initial transient had died out, the linear Landau damping regime was clearly established from which we determined the oscillation frequency and damping rate, $1.155\,\omega_{pe}$ and $0.0128\,\omega_{pe}$, respectively, which compare well with the corresponding values obtained from the Landau dispersion relation, namely 1.159 and $0.0126\,\omega_{pe}$. The time development of the electric field amplitude shows exact agreement with the work of Cheng and Knorr [1] (cf. their Fig. 1) and that of Canosa, Gazdag, and Fromm [2] (cf. their Fig. 3).

On increasing the initial field amplitude to $A = 0.5$ we represent the time evolution of the first three Fourier modes of the electric field in Fig. 1. Figure 2 shows the corresponding results obtained by Cheng and Knorr [1]. The first mode $|E_1|$ damps at a higher rate than that predicted by linear Landau theory ($\gamma_1 = -0.153$); using data lying between $t = 1.5\,\omega_{pe}^{-1}$ and $t = 8.7\,\omega_{pe}^{-1}$ we have $\gamma = -0.243$ which compares with the value of -0.281 found by Cheng and

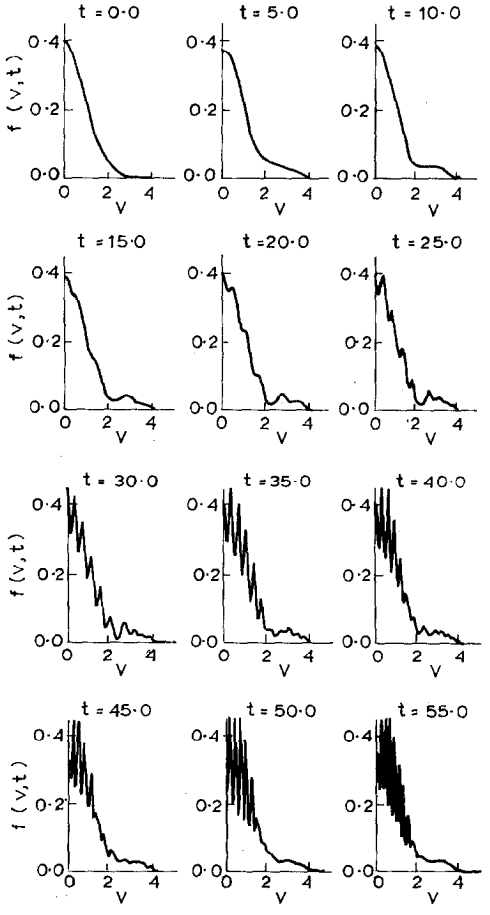

FIG. 3. Evolution of a distribution function.

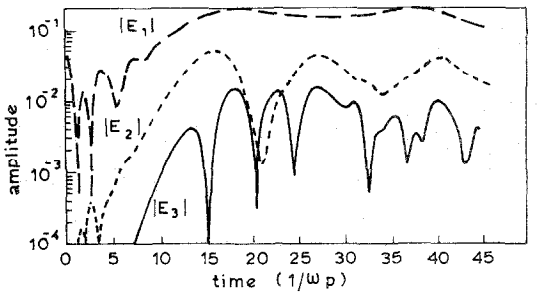

FIG. 4. Evolution of the first three electric field modes in the two-stream instability.

Knorr [1]. We also see that the first mode $|E_1|$ attains its first minimum at $t = 15.4\,\omega_{pe}^{-1}$, in good agreement with the values of $t = 15.3\,\omega_{pe}^{-1}$ observed by Cheng and Knorr [1] and $t = 15.4\,\omega_{pe}^{-1}$ observed by Canosa, Gazdag, and Fromm [2].

In Fig. 3 we show the time development of the spatially homogeneous part of the distribution function. In the initial stage a plateau is formed in the vicinity of the phase velocities of the wave at time $t = 10.0\,\omega_{pe}^{-1}$, in qualitative agreement with the predictions of the quasilinear theory. At $t = 15.0\,\omega_{pe}^{-1}$ a small bump appears in the tail of the distribution function at about the phase velocities of the modes and causes all of them to grow. Later a wave-like structure develops and grows on the main body of the distribution function and persists throughout the computation. As the amplitudes of the modes $|E_1|$, $|E_2|$, and $|E_3|$ grow (Fig. 2), the hole in the distribution function in the region $2.0 \leqslant v \leqslant 2.5$ becomes deeper, until $t = 30\,\omega_{pe}^{-1}$, following which it tends to be filled in. This is completed by $t = 40\,\omega_{pe}^{-1}$ at which time the first three modes saturate. The evolution of the distribution function

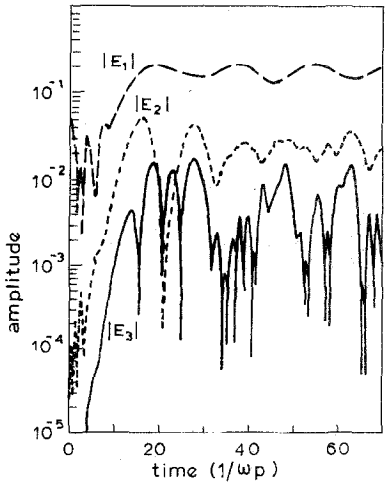

FIG. 5. Evolution of the first three electric field modes from the two-stream instability obtained by Cheng and Knorr [1].

observed in Fig. 3 agrees very closely indeed with the results obtained by Cheng and Knorr [1] (cf. their Fig. 5).

b. *The Two-Stream Instability*

As a second test problem we considered the classical two-stream instability. The actual problem studied involves two identical counterstreaming beams of electrons embedded in a neutralizing background. The initial electron distribution function has the form given in (1) multiplied by the factor v^2. The results are shown in Fig. 4 in which we chose plasma beam parameters to correspond to those used by both Cheng and Knorr [1] and Klimas [4]. In Fig. 4, the first three modes of the electric field are shown as functions of the time. The first mode E_1 after a transient phase, experiences exponential growth until it reaches its maximum at $t = 18.1\ \omega_{pe}^{-1}$. This mode then saturates and remains dominant at subsequent times. The second and third modes exhibit oscillatory behaviour after an initial transient phase. The behaviour of all three modes $|E_1|$, $|E_2|$, and $|E_3|$ agrees well with the observations of Klimas [4] (cf. his Fig. 3) and with the results obtained by Cheng and Knorr [1] reproduced in Fig. 5.

Figure 6 shows the electrostatic field energy as a function of time. The field energy grows from $t = 8.5$ to $t = 17.8\ \omega_{pe}^{-1}$, where it reaches its maximum and then oscillates with a period of about $18\ \omega_{pe}^{-1}$. For comparison the results obtained by Cheng and Knorr are also represented in Fig. 6 by the dashed curve.

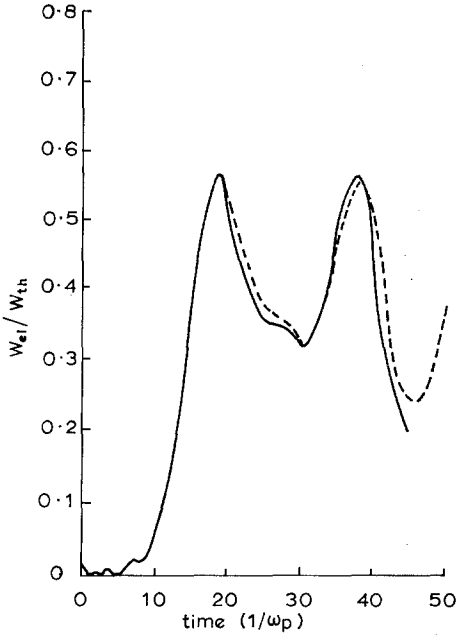

FIG. 6. Evolution of electrostatic field energy in the two-stream instability. The curve (---) shows for comparison the result obtained by Cheng and Knorr [1].

c. *The "Bump-on-Tail" Instability*

Finally, we tested our FEM code on the "bump-on-tail" instability studied by many authors both theoretically and computationally. In this problem electrons having a distribution function

$$f_e(x, v, o) = f_0(v)\left[1 + A \sum_{k=1}^{N} \cos K_0 x\right], \tag{2}$$

where

$$f_0(v) = (2\pi)^{-1/4}[h_0(v) + \sqrt{3/2}\, h_4(v)]\, e^{-v^2/2}$$

$$K_0 = 0.15, \qquad A = 0.006, \qquad N = 8$$

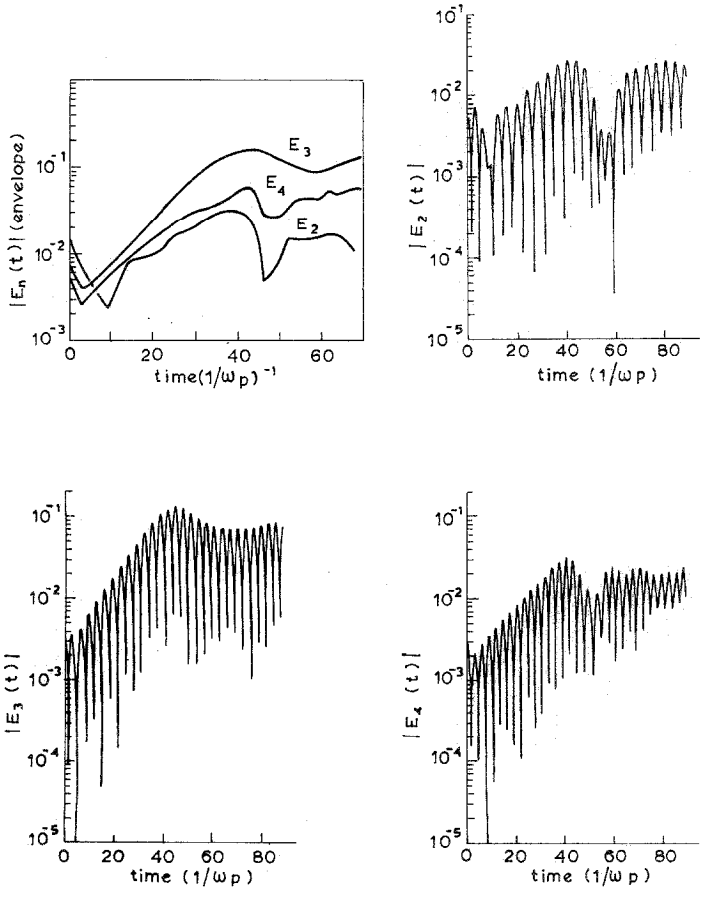

FIG. 7. Comparison of modes 2, 3, 4 for the bump-on-tail instability (b, c, d) with results (a) obtained by Armstrong and Montgomery [3].

and

$$h_m(v) = \frac{(-1)^m e^{v^2/2}}{(\sqrt{2\pi}\, m!)^{1/2}} \frac{d^m}{dv^m} e^{-v^2/2} \tag{3}$$

are embedded in a uniformly distributed immobile neutralizing background. In (3), h_m is the mth orthogonal Hermite polynomial.

In trial runs with $A = 0.006$, $|E_2|$, $|E_3|$, and $|E_4|$ are exponentially growing waves, with growth rates less than $0.1\,\omega_{pe}$, modes $|E_7|$ and $|E_8|$ are heavily Landau damped, and $|E_1|$, $|E_5|$, and $|E_8|$ are either marginally stable or weakly Landau damped. The behaviour of modes two to four is shown in Figs. 7b, c, d. The behaviour of the modes agrees well with the results of Armstrong and Montgomery [3], reproduced in Fig. 7a.

Turning to the velocity distribution we show in Fig. 8, $f(v, t)$ for $t = 0$, 15, 30, 45 ω_{pe}^{-1}. These results too are in good agreement with those found by Armstrong and Montgomery [3] and the velocity distributions computed by Dawson and Shanny [5]. All agree that the hole in the distribution fills in. However, there is no clear indication of the "plateau" predicted by quasilinear theory and no sign of the high energy tail of suprathermal particles seen by Dawson and Shanny.

We have also examined the evolution of the total electrostatic field energy. Our result is shown together with that of Armstrong and Montgomery [3] in Fig. 9. It is seen that once again very satisfactory agreement is obtained.

These tests demonstrate that the finite element Vlasov code can reproduce the various results of now-standard problems obtained by other authors using a range

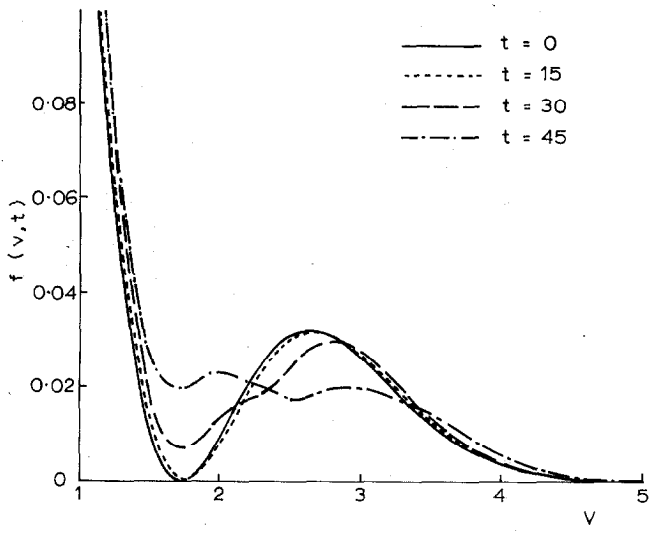

FIG. 8. Evolution of the bump-on-tail velocity distribution function.

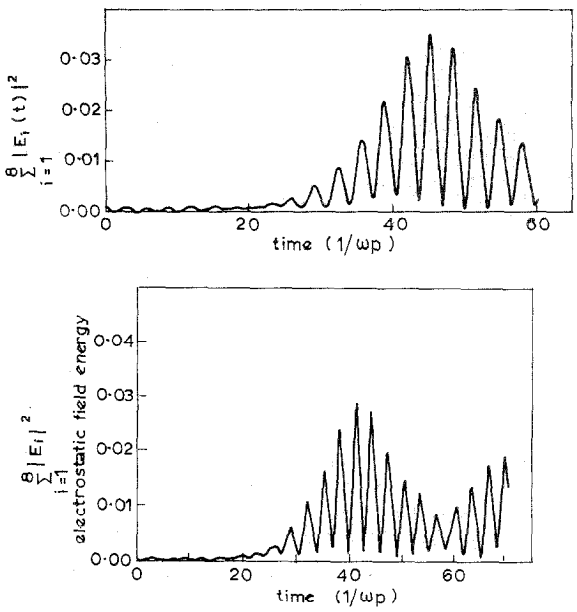

FIG. 9. Evolution of the electrostatic field energy (a) with the results (b) found by Armstrong and Montgomery [3] for comparison.

of methods. In the Landau damping run with a relatively large number of elements (256×32) and a time step of $t = 0.02\ \omega_{pe}^{-1}$, we obtained results identical with those reported by Cheng and Knorr [1] and Canosa, Gazdag, and Fromm [2]. The conservation of energy in these runs had an error as low as 10^{-5}. In studying the two stream instability, we used 128×16 elements and a time step of $t = 0.05\ \omega_{pe}^{-1}$ and found that the energy was conserved to better than 8×10^{-5}. For the "bump-on-tail" instability we used 128×16 elements and a time step of $t = 0.05\ \omega_{pe}^{-1}$. The conservation of energy was, in this case, better than 10^{-5}. These various comparisons have shown that the FEM Vlasov code performs satisfactorily in terms of accuracy and economy over a range of classical test problems. In these tests we have used periodic boundary conditions and fixed ions. However, the code has been written to cope both with non-periodic boundary conditions and mobile ions, both essential if we are to investigate a wider range of phenomena.

3. CONCLUSIONS

We conclude from this analysis that the FEM Vlasov code described in this work is a versatile tool for use in one-dimensional plasma problems. In practice the code has the following properties. In the first place noise levels are low and energy conservation accurate. Second, by using elements of varying size it is possible to cope

effectively with phenomena such as plasma sheaths within which the plasma parameters vary rapidly compared with their behaviour in the body of the plasma but sharp discontinuities or delta functions cannot be modelled. In principle there is no difficulty in extending the method to higher dimensions. In addition, the FEM code is well suited to dealing with complicated boundary geometry in problems where this has to be taken into account.

ACKNOWLEDGMENT

One of us (SIZ) wishes to acknowledge financial support from the Egyptian Ministry of Education.

REFERENCES

1. C. Z. CHENG AND G. KNORR, *J. Comput. Phys.* **22**, 330 (1976).
2. J. CANOSA, J. GAZDAG, AND J. E. FROMM, *J. Comput. Phys.* **15**, 34 (1974).
3. T. P. ARMSTRONG AND D. MONTGOMERY, *Phys. Fluids* **12**, 2094 (1969).
4. A. J. KLIMAS, *J. Comput. Phys.* **50**, 270 (1983).
5. J. M. DAWSON AND R. SHANNY, *Phys. Fluids* **11**, 1506 (1968).